SIAM J. APPL. MATH.
Vol. 80, No. 3, pp. 1356–1376

DEGENERATE PERIOD ADDING BIFURCATION STRUCTURE OF ONE-DIMENSIONAL BIMODAL PIECEWISE LINEAR MAPS*

JUAN SEGURA†, FRANK M. HILKER‡, AND DANIEL FRANCO§

Abstract. Motivated by a problem in the management of ecological populations, we study the bifurcation structure known as period adding structure for a family of one-dimensional bimodal piecewise linear maps. This structure is rather degenerate compared to the general case usually addressed in the literature. The degeneracy affects both the type of border collision bifurcations constituting the bifurcation structure and the number and location of the bifurcation points in the parameter space. We provide rigorous theoretical results that yield a complete description of the degenerate border collision bifurcations and a full determination of the bifurcation structure. This allows us to extend partial results previously reported about a similar problem. From an ecological point of view, we provide numerical simulations showing potential risks and opportunities associated with the bifurcation structure studied here. Moreover, we provide examples of applications of our results to some well-known population models, showing that the period adding structure ranges from very simple to very intricate.

Key words. nonsmooth discrete dynamical system, border collision bifurcation, periodicity region, continuum of periodic orbits, combined adaptive limiter control

AMS subject classifications. 37E05, 37N25, 37G35, 39A28

DOI. 10.1137/19M1251023

1. Introduction.

Actions in population management are often based on thresholds. For instance, when pests or nuisance species are too abundant, start harvesting them. If endangered species or game species become too rare, start restocking them. These threshold-based management actions lead to dynamical systems that are usually nonsmooth at the thresholds [9, 19, 23, 34, 35, 42, 43].

When parameters of a smooth system are varied in a certain direction in the parameter space, transitions between regular dynamics and chaos generally occur through a *route to chaos*, which consists of a certain sequence of bifurcations (for a review of these mechanisms see, for instance, [1]). However, in the case of nonsmooth systems these transitions may occur through a single bifurcation [8]. In this paper, we consider the case of one-dimensional (1D) piecewise smooth maps. These maps are characterized by the fact that the state space consists of several partitions separated by points at which the map is not differentiable, to which we will refer as *break points* or *kink points*. As parameters are varied, collisions between an invariant set

*Received by the editors March 20, 2019; accepted for publication (in revised form) April 13, 2020; published electronically May 28, 2020.
https://doi.org/10.1137/19M1251023
Funding: The work of the first author was supported by Osnabrück University. The work of the third author was supported by the UNED-ETSI Industriales, through project 2019-MAT11. The work of the first and third authors was supported by the Spanish Ministerio de Economía y Competitividad and FEDER through grant MTM2017-85054-C2-2-P.

†Departament d'Economia i Empresa, Universitat Pompeu Fabra, c/ Ramon Trias Fargas 25–27, 08005, Barcelona, Spain, and Departamento de Matemática Aplicada, E.T.S.I. Industriales, Universidad Nacional de Educación a Distancia (UNED), c/ Juan del Rosal 12, 28040, Madrid, Spain (joan.segura@upf.edu).

‡Institute of Mathematics and Institute of Environmental Systems Research, School of Mathematics/Computer Science, Osnabrück University, Barbarastr. 12, 49076 Osnabrück, Germany (frank.hilker@uni-osnabrueck.de).

§Departamento de Matemática Aplicada, E.T.S.I. Industriales, Universidad Nacional de Educación a Distancia (UNED), c/ Juan del Rosal 12, 28040, Madrid, Spain (dfranco@ind.uned.es).

and one of the break points can induce abrupt changes in the dynamics of piecewise smooth maps (e.g., the transition from an attracting fixed point to a chaotic attractor). These collisions correspond to the so-called border collision bifurcations (BCB), a term originally introduced by Nusse and Yorke [28]. This type of bifurcation can give rise to many structures that are completely different from scenarios occurring in smooth systems [4]. Several papers have studied these structures for certain families of maps (see, for instance, [17]).

In this paper, we consider a management problem from population biology, where the aim is to stabilize fluctuating population dynamics (in order to reduce extinction risk [11, 20, 24, 36] or to reduce variability in the yield [2, 6, 27, 38]). A recently introduced management strategy [37], combined adaptive limiter control (CALC), is based on two "adaptive" thresholds, where the population is harvested if it has increased too much and it is restocked if it has decreased too much. This management strategy is modeled by maps with two break points that split the state space into three partitions and make the maps bimodal. The outermost branches of the maps are determined by the control parameters and are linear. In the central partition of the state space, the control plays no role and the maps are given by the production function of the population, which may have any functional form (cf. Figure 1). A study of the performance of CALC in the management of different biological populations from several points of views (e.g., the enhancement of the stability or the prevention of population outbreaks) can be found in [37].

As already said, CALC is aimed at stabilizing fluctuating populations, which in many occasions can be described by unimodal maps with an unstable positive equilibrium. This is also the case we consider in this paper. For these population maps, the length of the central partition of the CALC map depends inversely on the control intensities. Thus, for high enough control intensities, given that the equilibrium acts as a repeller, the state variable is expected to leave the central partition of the state space after a certain period of time. For this reason, we focus our attention on the outermost partitions of the state space and study the bifurcation structure associated with the collision between the kink points and invariant sets lying in these

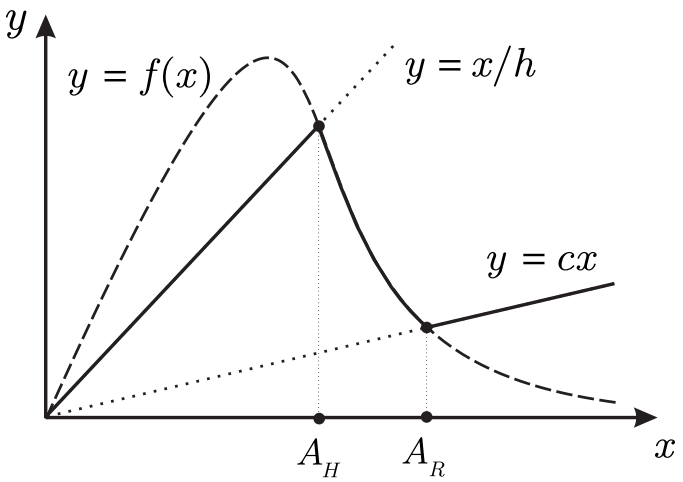

FIG. 1. *CALC function in the solid line, for a given production function f in the dashed line describing the underlying dynamics. The adaptive limiters are represented in the dotted line. A_H and A_R are breakpoints induced by the adaptive limiters.*

partitions. From the ecological point of view, there are also several reasons to study the outermost partitions of the state space. First, these partitions are more relevant to cases where the population size reaches rather small or large values, respectively corresponding to scenarios close to extinction or to population outbreaks. Second, the outermost partitions of the domain correspond to population sizes further away from the unstable positive equilibrium of the uncontrolled population. One may expect that this would make management more complicated because the situation is far from the uncontrolled scenario that may be the objective of the stabilization.

Since we consider only collisions with invariant sets lying in the outermost partitions of the state space, the dynamics of CALC at the bifurcation points are independent of the expression of the CALC map in the central partition, which corresponds to the production function of the population. Thus, for the description of the BCB of CALC we can replace the function in the central partition of the state space by a straight line joining the kink points of the map. This allows us to relate CALC to the broad existing literature about 1D piecewise linear (PWL) maps, which are characterized by all their branches being affine. These maps play a distinctive role among piecewise smooth maps and naturally appear in applied problems of a wide range of fields, e.g., circuit theory [13, 22, 44], economics [5, 16, 41], or cellular neural networks [10, 21, 26].

Many different bifurcation structures have been deeply studied for 1D piecewise maps with either affine (see, e.g., [3, 29, 30, 31]) or nonlinear (see, e.g., [3, 39, 40]) branches. Yet, the case corresponding to CALC is a special case of the former, since the outermost branches of the CALC map are linear, i.e., homogeneous. We show that the bifurcations observed for 1D bimodal PWL maps with the outermost branches linear correspond to a rather degenerate case of the already known bifurcation structure in the general case. The degeneracy of this case is twofold. First, the bifurcations that are observed constitute a degenerate case of BCBs that, to our knowledge, has not been studied yet. Second, the bifurcation structure, i.e., the number and location of the bifurcation points in the parameter space, also constitutes a degenerate case of the bifurcation structure of the general family of bimodal PWL maps. This degeneracy in the bifurcation structure (but not in the type of bifurcation) was previously reported by Foroni, Avellone, and Panchuk in [12] for a similar dynamical system, whose study was motivated by an economic model. Foroni, Avellone, and Panchuk [12] succeeded in providing a partial result for the determination of bifurcation points. That is, only a necessary but not sufficient condition for the occurrence of bifurcations was reported. This leaves the problem undetermined, since with just the condition provided in [12] the number of combinations of parameters for which a bifurcation could potentially occur is extremely high. This indetermination would imply serious difficulties in the ecological problem motivating this paper, since finding control intensities away from any potential bifurcation would be difficult or even impossible with just the condition given in [12]. In this sense, it is of practical interest to exactly determine which combinations of parameter values correspond to bifurcation points and which ones do not.

Of course, this requires finding a necessary and sufficient condition for the occurrence of the considered bifurcations. We provide and prove such a condition not only for CALC and for the problem considered in [12] but for a broader family of maps that covers all the cases in which the degenerate bifurcations under study take place. By using that condition, we fully determine the bifurcation structure of CALC and complete the analytical description of the bifurcation structure of the family of maps considered in [12]. Regarding the degenerate bifurcations studied in this paper, we

provide a complete theoretical description. We prove that a continuum of cycles lying on the outermost partitions of the state space emerge at the bifurcation points, while in the nondegenerate case a unique cycle satisfying that condition exists. We also show that no cycles of this kind exist at either side of the bifurcation points.

As an application of the above results, we provide numerical simulations of populations managed by CALC for some well-known models in discrete-time population dynamics, namely the Ricker [32] and Hassell [18] models. These simulations show that at the bifurcation points the continuum of cycles appears to attract all possible orbits except those corresponding to fixed points. This has important implications from the practical point of view. In the case that managers are interested in keeping populations away from bifurcation points but this is not possible, the results provided here allow them to know in advance which dynamical behavior can be expected for the managed populations. Additionally, these examples show that the bifurcation structure for CALC strongly depends on the underlying dynamics and ranges from very simple to very intricate.

2. Combined adaptive limiter control. We start by describing and modeling CALC, followed by a description of abrupt transitions between different attractors that may occur in the dynamics of populations managed by that strategy.

2.1. Description of the general dynamic model. Populations managed by CALC can be either restocked or harvested depending on the population size. If the population size x_t at time step t grows beyond a certain proportion x_t/h with $h \in (0,1)$, the population is harvested and its size is reset to this proportion. If the population size declines below another proportion cx_t with $c \in (0,1)$, the population is restocked and its size is reset to this proportion. This two-parameter strategy combines the one-parameter strategies of adaptive limiter control [34] and adaptive threshold harvesting [35]. To obtain a mathematical model for CALC, we denote by b_t the population size at time step t before the control intervention and by a_t the population size after intervention. The dynamics of populations managed by CALC are given by the system of difference equations

$$\begin{aligned} b_{t+1} &= f(a_t), \\ a_{t+1} &= \begin{cases} ca_t, & b_{t+1} < ca_t, \\ b_{t+1}, & ca_t \le b_{t+1} \le a_t/h, \\ a_t/h, & b_{t+1} > a_t/h, \end{cases} \end{aligned} \tag{2.1}$$

where f is the production function of the uncontrolled population and $c, h \in (0,1)$ are the restocking and harvesting intensities, respectively. Substituting the value of b_{t+1} into the second equation of (2.1), the dynamics of populations managed by CALC are described by the piecewise 1D difference equation

$$a_{t+1} = \begin{cases} ca_t, & f(a_t) < ca_t, \\ f(a_t), & ca_t \le f(a_t) \le a_t/h, \\ a_t/h, & f(a_t) > a_t/h. \end{cases}$$

The effect of CALC on a specific population model is shown in Figure 2. Similarly to adaptive limiter control [14, 15, 33, 34, 42] and adaptive threshold harvesting [35, 36], we observe that CALC is able to reduce the range of fluctuations in the population size.

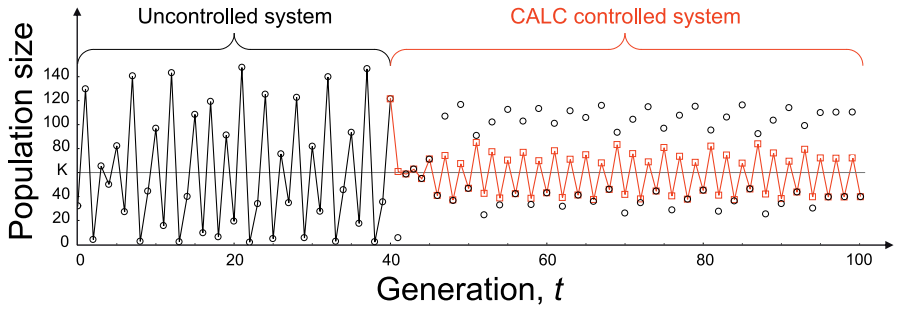

FIG. 2. *During the first* 40 *generations the population is uncontrolled and its dynamics are described by the Ricker map* $f(x) = x\exp(r(1 - x/K))$ *with* $r = 3$ *and* $K = 60$. *In the next* 60 *generations, the population is managed by CALC with intensities* $c = 0.5$ *and* $h = 0.55$. *Black circles correspond to the population size before the control intervention, and red squares after intervention.*

2.2. CALC of unimodal population maps. We will assume that the underlying population dynamics are given by a first-order 1D difference equation of the form

$$x_{t+1} = f(x_t),\ x_0 \in [0, +\infty),\ t \in \mathbb{N}, \tag{2.2}$$

with f satisfying the following conditions:

(C1) $f : [0, +\infty) \to [0, +\infty)$ is continuously differentiable and such that $f(x) > 0$ for all $x \in (0, +\infty)$.

(C2) f has two nonnegative fixed points $x = 0$ and $x = K > 0$, with $f(x) > x$ for $0 < x < K$ and $f(x) < x$ for $x > K$.

(C3) f has a unique critical point $d \in (0, K)$ in such a way that $f'(x) > 0$ for all $x \in (0, d)$, $f'(x) < 0$ for all $x \in (d, +\infty)$, and $f'(0^+) \in \mathbb{R}$.

(C4) f is concave downward in $(0, d)$.

These conditions describe a hump-shaped production function peaking at $x = d$ with two fixed points, namely (i) the extinction state $x = 0$ and (ii) a positive equilibrium $x = K$, which corresponds to the carrying capacity of the population. Biologically speaking, the dynamics are overcompensatory with no demographic Allee effect. Many common models satisfy these conditions, e.g., the Ricker [32], Hassell [18], or generalized Beverton–Holt [7] models, which are suitable to model populations with a pronounced reproductive cycle.

Assuming conditions (C1)–(C4), CALC combines both restocking and harvesting for given $(c, h) \in (0, 1) \times (0, 1)$ only when the two straight lines $y = cx$ and $y = x/h$ have nonzero intersections with the curve $y = f(x)$. This happens only when the harvesting intensity is high enough, namely $h > \inf_{x\in(0,+\infty)} x/f(x)$. In what follows, we will assume that this condition is met. Under this assumption, there is a unique nonzero intersection between $y = x/h$ and $y = f(x)$, whose abscissa we denote by A_H. Similarly, for all $c \in (0, 1)$ there is a unique nonzero intersection between $y = cx$ and $y = f(x)$, whose abscissa we denote by A_R. Moreover, given that $c < 1 < 1/h$, these two points are always different and satisfy $A_H < K < A_R$ (cf. Figure 1). With this, the dynamics of populations subject to CALC are described by the difference equation $x_{t+1} = F(x_t)$, where $F\colon [0, +\infty) \to [0, +\infty)$ is the piecewise function given by

$$F(x) = \begin{cases} x/h, & 0 \le x \le A_H, \\ f(x), & A_H < x < A_R, \\ cx, & x > A_R. \end{cases} \tag{2.3}$$

Function F is bimodal since it increases for $x < \max\{d, A_H\}$, then decreases for $\max\{d, A_H\} < x < A_R$, and increases again on the rest of the domain. Moreover, the functional form of the two outermost branches of F (the first ranging from 0 to A_H and the last from A_R to $+\infty$) are independent of the underlying population production function and are determined by the control intensities. Yet, the population map f defines the length of each of these branches.

2.3. Transitions induced by the combination of restocking and harvesting. The stabilizing properties of CALC can be observed in Figure 3 for the Ricker map $f(x) = x\exp(r(1-x/K))$ with $r = 3$ and $K = 60$, where the restocking intensity is set at $c = 0.6$ and the harvesting intensity is varied. For low harvesting intensities ($h \lesssim 0.4$), restocking prevails and the reduction in the fluctuation range (i.e., the difference between the asymptotic maximum and minimum population sizes) is only due to restocking (for the uncontrolled system, the asymptotic population size ranges from

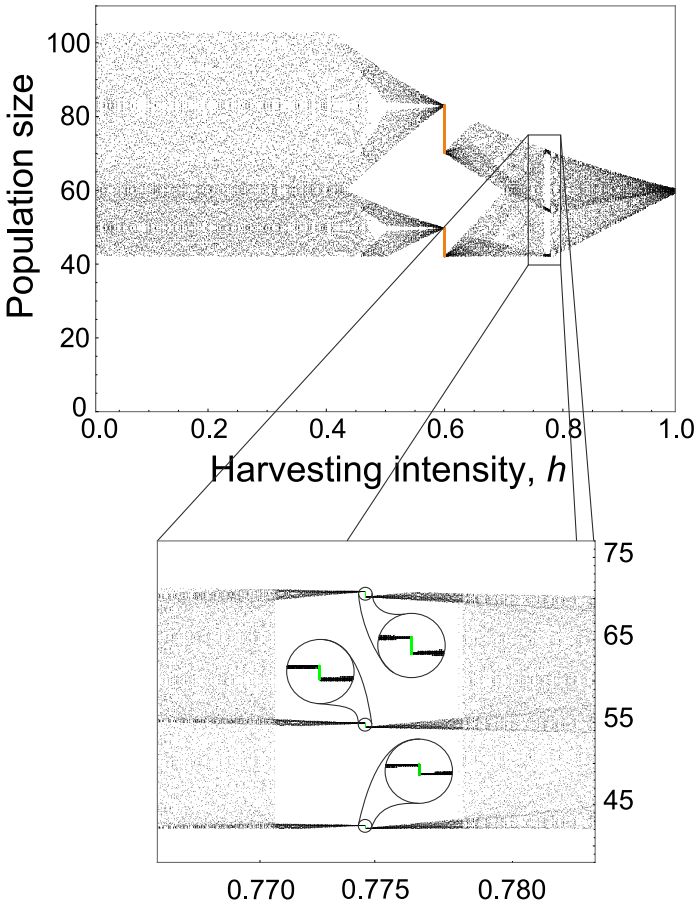

FIG. 3. *Bifurcation diagram for CALC with $c = 0.6$ and varying h. The underlying population dynamics are given by the Ricker map $f(x) = x\exp(r(1-x/K))$ with $r = 3$ and $K = 60$. For each value of h, black dots represent 30 iterates of the state variable after a transient of 10,000 iterates with initial conditions obtained as pseudorandom real numbers in the interval $(0, f(d)]$. For $h = 0.6$ and $h = \sqrt{0.6}$, iterates were obtained for 1,000 different initial conditions, which are respectively represented by orange and green dots.*

$f^2(d) \approx 1.834$ to $f(d) \approx 147.781$). For high enough harvesting intensities ($h \gtrsim 0.4$), the fluctuation range decreases as h increases. A similar behavior is observed for fixed h and varying c (not shown here).

In addition to the stabilizing effect of CALC, Figure 3 shows another important fact that is the focus of this paper. For certain combinations of the control parameters (e.g., $c = h = 0.6$), abrupt jumps between different attractors are observed. Interestingly, such a behavior is inherent to the combination of restocking and harvesting, since it is not observed when only restocking [14, 34] or only harvesting [35] are considered. This suggests that around the critical points in the parameter space for which these phenomena occur, slight variations in the control intensities may have severe consequences in the managed populations, which we elaborate on in the following.

From the ecological point of view, the population size undergoes a sharp change. As Figure 3 shows, the attractors on different sides of the critical points may correspond to significantly different population sizes. This is also reflected in the average population size (cf. Figure 4). Such a transition can seriously affect the stability and persistence of the managed populations in certain situations. This would be the case, for instance, for populations at risk of extinction. In such a case, a sharp shift from an attractor to another corresponding to lower population sizes could threaten the population persistence. By contrast, such a transition could be beneficial in the case of nuisance or invasive species.

There are several implications that these abrupt changes in the dynamics may have from a management point of view. As can be observed in Figure 4, the transition between different attractors entails a sharp change in the number of individuals that are restocked or harvested. On one side of the critical point in the parameter space the intervention is essentially based on restocking and few individuals are harvested. By contrast, on the other side, only few individuals are restocked and harvesting prevails. Logically, such a transition may have severe consequences on the cost and yield of the intervention. For instance, in the case of exploited populations, shifting from mostly harvesting to mostly restocking drastically reduces the yield and increases the cost of

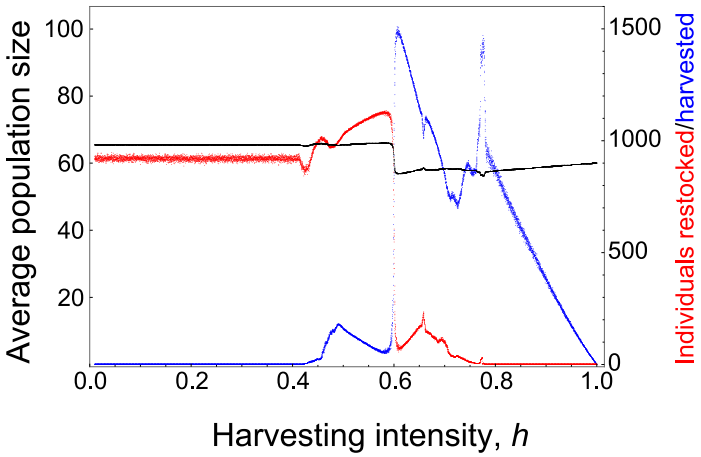

FIG. 4. *For CALC with a fixed restocking intensity* $c = 0.6$ *and varying the harvesting intensity, the black dots represent the asymptotic average population size during* 100 *generations, the red dots represent the asymptotic number of restocked individuals, and the blue dots represent the asymptotic number of harvested individuals. All values are averaged over* 50 *replicates. The underlying population dynamics are given by the Ricker map* $f(x) = x\exp(r(1-x/K))$ *with* $r = 3$ *and* $K = 60$.

the exploitation. Of course, this would also imply serious problems with respect to the organization, planning, and preparation of the intervention, since it would have to be completely overhauled, provided that the necessary resources are available at all.

3. Bifurcation structure. The aim of this section is to study the bifurcation structure associated with the abrupt changes in the dynamics of populations managed by CALC that were observed in the previous section. To that end, as said in the introduction, we relate CALC to general 1D bimodal PWL maps. We start by introducing the family of these maps and showing that the maps with the outermost branches being linear like the CALC map constitute a strict subfamily. Next, we provide necessary and sufficient conditions for the occurrence of certain BCBs in terms of the parameters for this subfamily. Finally, we study the dynamics at the bifurcation points.

3.1. Border collision bifurcations and period adding structure of general 1D continuous bimodal piecewise linear maps. One-dimensional continuous bimodal PWL maps can be written in the form

$$F(x) = \begin{cases} F_{\mathcal{L}}(x) = a_{\mathcal{L}}x + \mu_{\mathcal{L}}, & 0 \le x \le d_{\mathcal{L}}, \\ F_{\mathcal{M}}(x) = a_{\mathcal{M}}x + \mu_{\mathcal{M}}, & d_{\mathcal{L}} < x < d_{\mathcal{R}}, \\ F_{\mathcal{R}}(x) = a_{\mathcal{R}}x + \mu_{\mathcal{R}}, & x \ge d_{\mathcal{R}}, \end{cases} \tag{3.1}$$

with $a_{\mathcal{M}}, \mu_{\mathcal{L}}, \mu_{\mathcal{M}}, \mu_{\mathcal{R}} \in \mathbb{R}$ and $d_{\mathcal{L}}, d_{\mathcal{R}}, a_{\mathcal{L}}, a_{\mathcal{R}} \in (0, +\infty)$. In what follows, we will denote the outermost partitions of the domain of F by $I_{\mathcal{L}} = [0, d_{\mathcal{L}}]$ and $I_{\mathcal{R}} = [d_{\mathcal{R}}, +\infty)$.

Notice that (3.1) depends on eight parameters, but two of them can always be obtained from the others by imposing continuity. Since the commonality between CALC and (3.1) is in the outermost branches, we will assume that $a_{\mathcal{M}}$ and $\mu_{\mathcal{M}}$ are determined in terms of $a_{\mathcal{L}}$, $a_{\mathcal{R}}$, $\mu_{\mathcal{L}}$, $\mu_{\mathcal{R}}$, $d_{\mathcal{L}}$, and $d_{\mathcal{R}}$. In what follows, we will denote by $\mathcal{F}$ the resulting six-parametric family of maps. Considering only the outermost partitions of the state space, the CALC map (2.3) in terms of the control intensities c and h can be considered as a biparametric subfamily $\mathcal{F}_1 \subset \mathcal{F}$ under certain parameter restrictions. First, the linearity of the outermost branches of (2.3) implies $\mu_{\mathcal{L}} = 0$ and $\mu_{\mathcal{R}} = 0$. Second, the two kink points $d_{\mathcal{L}} = A_H$ and $d_{\mathcal{R}} = A_R$ of (2.3) are uniquely determined in terms of c and h by the equalities $f(d_{\mathcal{L}}) = a_{\mathcal{L}}d_{\mathcal{L}}$ and $f(d_{\mathcal{R}}) = a_{\mathcal{R}}d_{\mathcal{R}}$, where $a_{\mathcal{L}} = 1/h$ and $a_{\mathcal{R}} = c$.

As parameters are varied, periodic orbits of (3.1) can collide with either $d_{\mathcal{L}}$ or $d_{\mathcal{R}}$. This gives rise to three different bifurcation structures depending on which partitions of the state space contain points of these cycles [31]:

- *Skew tent map structure:* the points of the cycles are located on two adjacent partitions of the state space.
- *Period adding structure:* the points of the cycles are located on the outermost partitions of the state space.
- *Fin structure:* the points of the cycles are located on all three partitions of the state space.

As already mentioned, we restrict our study to border collisions caused by invariant sets lying in the outermost partitions of the state space, and thus we focus on BCBs associated with the period adding structure (PAS). The elements of this structure are called *periodicity regions* (also known as *Arnold tongues* or *mode-locking tongues*) and are regions in the parameter space for which there exist cycles with all their points lying in $I_{\mathcal{L}} \cup I_{\mathcal{R}}$. Two periodicity regions differ in the number of points of their cycles in $I_{\mathcal{L}}$ and $I_{\mathcal{R}}$.

The PAS for $\mathcal{F}$ can be determined in terms of the *rotation numbers* of the associated cycles [31]. If a cycle lying in $I_{\mathcal{L}} \cup I_{\mathcal{R}}$ has m points in $I_{\mathcal{L}}$ and n points in $I_{\mathcal{R}}$, we define its rotation number as the rational number $\rho = {}^{m}/_{(n+m)}$, i.e., the number of points in the leftmost partition of the state space divided by the period of the cycle. Two rotation numbers $\rho_1 = {}^{m_1}/_{p_1}$ and $\rho_2 = {}^{m_2}/_{p_2}$ are Farey neighbors when $|m_1 p_2 - m_2 p_1| = 1$, and their Farey sum is defined as $\rho_1 \oplus \rho_2 = {}^{(m_1+m_2)}/_{(p_1+p_2)}$. Using these definitions, the order and existence of the periodicity regions of $\mathcal{F}$ are completely determined by the following rule: if two periodicity regions are associated with cycles with Farey neighbor rotation numbers ρ_1 and ρ_2, then in the parameter space between them there exists another periodicity region related to cycles with rotation number $\rho_1 \oplus \rho_2$. It is because of this rule that the bifurcation structure is called *period adding*. Based on this principle, the PAS of $\mathcal{F}$ was iteratively determined in [31] by using Leonov's approach [17, 25]. Given a rotation number, the corresponding periodicity region is a portion of the 6D parameter space bounded by two different manifolds, which are derived by imposing the collision of each of the kink points of (3.1) with cycles of that rotation number.

3.2. Determining border collision bifurcation points under certain homogeneity conditions. Since $\mathcal{F}_1 \subset \mathcal{F}$, it would be logical to think that one could obtain a complete description of the PAS of $\mathcal{F}_1$ by substituting the parameter restrictions defining this subfamily into the already known expressions for the periodicity regions of $\mathcal{F}$. Unfortunately, we will see that this is not the case. This idea was used in [12] for another biparametric subfamily of maps $\mathcal{F}_2 \subset \mathcal{F}$ given by the parameter restrictions $\mu_{\mathcal{L}} = 0$, $\mu_{\mathcal{R}} = 0$, $a_{\mathcal{L}} + a_{\mathcal{R}} = 2$, and $2d_{\mathcal{L}}d_{\mathcal{R}} - d_{\mathcal{L}} - d_{\mathcal{R}} = 0$. Notice that two of these restrictions, $\mu_{\mathcal{L}} = 0$ and $\mu_{\mathcal{R}} = 0$, are common with $\mathcal{F}_1$. If we consider only these two restrictions, we obtain a four-parametric subfamily $\mathcal{F}_0 \subset \mathcal{F}$ that includes both $\mathcal{F}_1$ and $\mathcal{F}_2$ as strict subfamilies. Consider a rotation number ${}^{m}/_{(n+m)}$. It could be expected that when the two restrictions for $\mathcal{F}_0$ were substituted into the equations of the two manifolds $\xi_{\mathcal{L}}$ and $\xi_{\mathcal{R}}$ bounding the corresponding periodicity region of $\mathcal{F}$ (which, recall, lie in a 6D space), they would lead to another two manifolds in the 4D parameter space of $\mathcal{F}_0$. In that case, the periodicity region of $\mathcal{F}_0$ for the given rotation number would be the parameter space between these two manifolds. However, when $\mu_{\mathcal{L}} = 0$ and $\mu_{\mathcal{R}} = 0$ are substituted into the equations of $\xi_{\mathcal{L}}$ and $\xi_{\mathcal{R}}$ not only $\mu_{\mathcal{L}}$ and $\mu_{\mathcal{R}}$ vanish, but also $d_{\mathcal{L}}$ and $d_{\mathcal{R}}$ drop from the equations. To illustrate this consider, for instance, $m = 1$. In that case, the equations of $\xi_{\mathcal{L}}$ and $\xi_{\mathcal{R}}$ after imposing $\mu_{\mathcal{L}} = \mu_{\mathcal{R}} = 0$ are given by [12]

$$\xi_{\mathcal{L}} : \frac{(1 - a_{\mathcal{L}} a_{\mathcal{R}}^n)\, d_{\mathcal{L}}}{a_{\mathcal{R}}^n} = 0,$$

$$\xi_{\mathcal{R}} : \frac{(1 - a_{\mathcal{L}} a_{\mathcal{R}}^n)\, d_{\mathcal{R}}}{a_{\mathcal{R}}^{n-1}} = 0.$$

As can be observed, $d_{\mathcal{L}}$ and $d_{\mathcal{R}}$ are irrelevant in these equations and $\xi_{\mathcal{L}}$ and $\xi_{\mathcal{R}}$ are reduced to a unique manifold in the 4D parameter space of $\mathcal{F}_0$, which is given by $a_{\mathcal{L}} a_{\mathcal{R}}^n = 1$. This last condition can be generalized to $a_{\mathcal{L}}^m a_{\mathcal{R}}^n = 1$ for a generic rotation number ${}^{m}/_{(n+m)}$ [12]. This means that the PAS of $\mathcal{F}_0$ is rather degenerate with respect to the one of $\mathcal{F}$, since all periodicity regions of $\mathcal{F}_0$ have null Lebesgue measure in its parameter space. In particular, all points in a periodicity region of $\mathcal{F}_0$ are bifurcation points, i.e., for all of them at least one of the kink points is in a cycle with all its points in the outermost partitions of the state space.

The main inconvenience of the fact that $d_{\mathcal{L}}$ and $d_{\mathcal{R}}$ drop from the equations of $\xi_{\mathcal{L}}$ and $\xi_{\mathcal{R}}$ when the restriction $\mu_{\mathcal{L}} = \mu_{\mathcal{R}} = 0$ is imposed is that the condition that is obtained after substitution, $a_{\mathcal{L}}^m a_{\mathcal{R}}^n = 1$, is necessary but not sufficient for the occurrence of BCBs of the PAS of $\mathcal{F}_0$. Indeed, $d_{\mathcal{L}}$ and $d_{\mathcal{R}}$ actually play a central role in the problem. Assume that the four parameters defining $\mathcal{F}_0$ are set at values satisfying $d_{\mathcal{L}} < \min\{a_{\mathcal{R}} d_{\mathcal{R}}, d_{\mathcal{R}}/a_{\mathcal{L}}\}$, $a_{\mathcal{L}} > 1$, $0 < a_{\mathcal{R}} < 1$, and $a_{\mathcal{L}}^m a_{\mathcal{R}}^n = 1$ for certain $n, m \in \mathbb{N}$. According to the last equality, we could expect that a BCB of the PAS of $\mathcal{F}_0$ occurred for these values, i.e., that either $d_{\mathcal{L}}$ or $d_{\mathcal{R}}$ was in a cycle with all its points in $I_{\mathcal{L}} \cup I_{\mathcal{R}}$. However, this is not possible since $d_{\mathcal{L}} < F_{\mathcal{L}}(d_{\mathcal{L}}) = a_{\mathcal{L}} d_{\mathcal{L}} < d_{\mathcal{R}}$ and $d_{\mathcal{L}} < F_{\mathcal{R}}(d_{\mathcal{R}}) = a_{\mathcal{R}} d_{\mathcal{R}} < d_{\mathcal{R}}$.

If the PAS of $\mathcal{F}_0$ cannot be completely determined by direct substitution of its parameter restrictions into the PAS of $\mathcal{F}$, neither can the PAS of any subfamily of $\mathcal{F}_0$ like the $\mathcal{F}_1$ considered here or the $\mathcal{F}_2$ considered in [12]. This was implicitly observed for $\mathcal{F}_2$ in [12] when it was shown that in some specific cases no BCB can occur even if the condition $a_{\mathcal{L}}^m a_{\mathcal{R}}^n = 1$ is met. Yet, no complete description of the PAS of $\mathcal{F}_2$ in terms of the parameters was obtained. With the following result, which yields a necessary and sufficient condition for the occurrence of BCBs of the PAS of $\mathcal{F}_0$, we will complete this description and fully determine the PAS of CALC.

PROPOSITION 3.1. *A boundary collision bifurcation of the period adding structure of* (3.1) *with* $\mu_{\mathcal{L}} = \mu_{\mathcal{R}} = 0$ *occurs if and only if there exist* $\lambda \in (0,1)$ *and* $m, n \in \mathbb{N}$ *with* $\gcd(m,n) = 1$ *such that* $a_{\mathcal{L}} = \lambda^{-n}$, $a_{\mathcal{R}} = \lambda^m$, *and* $\lambda d_{\mathcal{R}} \le d_{\mathcal{L}}$. *Moreover, the two kink points* $d_{\mathcal{L}}$ *and* $d_{\mathcal{R}}$ *are* $(m+n)$*-periodic and their orbits have* m *points in* $I_{\mathcal{L}}$ *and* n *points in* $I_{\mathcal{R}}$.

Proof. Assume that a BCB of the PAS of (3.1) with $\mu_{\mathcal{L}} = \mu_{\mathcal{R}} = 0$ occurs. Then, either $d_{\mathcal{L}}$ or $d_{\mathcal{R}}$ must be in a cycle $\mathcal{O}$ with all its points in $I_{\mathcal{L}} \cup I_{\mathcal{R}}$. Assume that this cycle has m points in $I_{\mathcal{L}}$ and n points in $I_{\mathcal{R}}$. Since $F_{\mathcal{L}}(x) = a_{\mathcal{L}} x$ and $F_{\mathcal{R}}(x) = a_{\mathcal{R}} x$ commute under composition, if $d_{\mathcal{L}} \in \mathcal{O}$ then $a_{\mathcal{L}}^m a_{\mathcal{R}}^n d_{\mathcal{L}} = d_{\mathcal{L}}$. Similarly, $d_{\mathcal{R}} \in \mathcal{O}$ leads to $a_{\mathcal{L}}^m a_{\mathcal{R}}^n d_{\mathcal{R}} = d_{\mathcal{R}}$. Given that $0 < d_{\mathcal{L}} < d_{\mathcal{R}}$, the terms $d_{\mathcal{L}}$ and $d_{\mathcal{R}}$ can be canceled from these equalities, after which both of them lead to the same condition $a_{\mathcal{L}}^m a_{\mathcal{R}}^n = 1$. In the case that $a_{\mathcal{L}} < 1$, all orbits starting in $I_{\mathcal{L}}$ would stay in $I_{\mathcal{L}}$ and monotonically converge to 0, which contradicts the occurrence of a BCB. Therefore, it must be $a_{\mathcal{L}} > 1$ and $0 < a_{\mathcal{R}} < 1$. Then, if we set $\lambda = a_{\mathcal{R}}^{1/m} \in (0,1)$ it follows that $a_{\mathcal{L}} = \lambda^{-n}$ and $a_{\mathcal{R}} = \lambda^m$. On the other hand, if $\gcd(m,n) = d > 1$, then $m/d \in \mathbb{N}$, $n/d \in \mathbb{N}$, and $a_{\mathcal{L}}^{-m/d} a_{\mathcal{R}}^{n/d} = 1$, and thus $m+n$ is not the prime period of $\mathcal{O}$. Consequently, we can assume $\gcd(m,n) = 1$.

Suppose that $d_{\mathcal{R}} \in \mathcal{O}$. Since $\mathcal{O} \subset (I_{\mathcal{L}} \cup I_{\mathcal{R}})$, any point of $\mathcal{O}$ can be obtained by starting at $d_{\mathcal{R}}$ and successively applying $F_{\mathcal{R}}(x) = \lambda^m x$ a certain number p of times and $F_{\mathcal{L}}(x) = \lambda^{-n} x$ another certain number q of times in a specific order, with $p \in \{0, \dots, n-1\}$ and $q \in \{0, \dots, m-1\}$. Given that $F_{\mathcal{R}}$ and $F_{\mathcal{L}}$ commute under composition, all the points of $\mathcal{O}$ can be expressed in the form $\lambda^{pm-qn} d_{\mathcal{R}}$ for certain p and q in the aforementioned ranges. Since m and n are coprime, using Bezout's lemma we can find p and q such that $pm - qn = 1$. Thus, $\lambda d_{\mathcal{R}} \in \mathcal{O}$. On the other hand, given that $\lambda d_{\mathcal{R}} < d_{\mathcal{R}}$ and $\mathcal{O} \subset (I_{\mathcal{L}} \cup I_{\mathcal{R}})$, it follows that $\lambda d_{\mathcal{R}} \in I_{\mathcal{L}}$, and thus $\lambda d_{\mathcal{R}} \le d_{\mathcal{L}}$. The same condition is derived when repeating these arguments for the case $d_{\mathcal{L}} \in \mathcal{O}$.

Assume now that there exist $\lambda \in (0,1)$ and $m, n \in \mathbb{N}$ with $\gcd(m,n) = 1$ such that $a_{\mathcal{L}} = \lambda^{-n}$, $a_{\mathcal{R}} = \lambda^m$, and $\lambda d_{\mathcal{R}} \le d_{\mathcal{L}}$. We will prove that the set $\mathcal{U} = \{\lambda^i d_{\mathcal{R}}\}_{i=1-n}^{m}$ is an $(m+n)$-cycle that has m points in $I_{\mathcal{L}}$ and n points in $I_{\mathcal{R}}$. Consider $\mathcal{U}_{\mathcal{L}} = \{\lambda^i d_{\mathcal{R}}\}_{i=1}^{m}$

and $\mathcal{U}_\mathcal{R} = \{\lambda^i d_\mathcal{R}\}_{i=1-n}^{0}$. With this notation, $\mathcal{U} = \mathcal{U}_\mathcal{L} \cup \mathcal{U}_\mathcal{R}$, $\mathcal{U}_\mathcal{L} \subset I_\mathcal{L}$, and $\mathcal{U}_\mathcal{R} \subset I_\mathcal{R}$. Given that $\lambda < 1$, $F(x) = F_\mathcal{L}(x) = \lambda^{-n}x > x$ for $x \in \mathcal{U}_\mathcal{L}$ and $F(x) = F_\mathcal{R}(x) = \lambda^m x < x$ for $x \in \mathcal{U}_\mathcal{R}$. Besides, $F(\max\mathcal{U}_\mathcal{L}) = F(\lambda d_\mathcal{R}) = \lambda^{1-n} d_\mathcal{R} = \max\mathcal{U}$ and $F(\min\mathcal{U}_\mathcal{R}) = F(d_\mathcal{R}) = \lambda^m d_\mathcal{R} = \min\mathcal{U}$. This proves that $\mathcal{U}$ is an invariant set for F.

Suppose now that $F^q(x) = x$ for certain $x \in \mathcal{U}$ and $q \in \mathbb{N}$. Since $\mathcal{U}$ is F-invariant, it follows that $\{x, F(x), \dots, F^{q-1}(x)\} \subset (I_\mathcal{L} \cup I_\mathcal{R})$. Assume that $\tilde{m}$ of these points lies in $I_\mathcal{L}$ and $\tilde{n}$ in $I_\mathcal{R}$. Then, by the commutativity between $F_\mathcal{L}$ and $F_\mathcal{R}$, it follows that $F^q(x) = \lambda^{m\tilde{n}-n\tilde{m}}x = x$, which implies $m\tilde{n} = n\tilde{m}$. Since m and n are coprime, this equality is only possible if $\tilde{m}$ is a multiple of m and $\tilde{n}$ is a multiple of n. Assume that $\tilde{m} = km$ for a certain $k \in \mathbb{N}$. Then, $\tilde{n} = kn$ and $q = \tilde{m} + \tilde{n} = k(m+n) \geq m+n$. This implies that the $m+n$ points of the set $\mathcal{V} = \{d_\mathcal{R}, F(d_\mathcal{R}), \dots, F^{m+n-1}(d_\mathcal{R})\} \subseteq \mathcal{U}$ are all different, and thus $\mathcal{V} = \mathcal{U}$. Since m points of $\mathcal{U}$ lie in $I_\mathcal{L}$ and n lie in $I_\mathcal{R}$, again by the commutativity between $F_\mathcal{L}$ and $F_\mathcal{R}$, it follows that $F^{m+n}(d_\mathcal{R}) = (\lambda^{-n})^m(\lambda^m)^n d_\mathcal{R} = d_\mathcal{R}$. This proves that $d_\mathcal{R}$ is in an $(m+n)$-cycle that has m points in $I_\mathcal{L}$ and n points in $I_\mathcal{R}$ and thus, in particular, a BCB of the PAS of (3.1) occurs for the considered parameter values. The same conclusion can be drawn for the kink point $d_\mathcal{L}$ by applying the same arguments to the set $\tilde{\mathcal{U}} = \{\lambda^i d_\mathcal{L}\}_{i=-n}^{m-1}$. ∎

Interestingly, for the family $\mathcal{F}$ BCBs can occur for any positive values of $a_\mathcal{L}$ and $a_\mathcal{R}$ [30]. However, Proposition 3.1 shows that for the subfamily $\mathcal{F}_0$ they can only take place for $a_\mathcal{L} > 1$ and $0 < a_\mathcal{R} < 1$. On the other hand, Proposition 3.1 resolves the degeneracy in the PAS of $\mathcal{F}$ that emerges when the homogeneity of the outermost branches of the maps is imposed. In particular, this result determines the PAS of any subfamily of $\mathcal{F}$ contained in $\mathcal{F}_0$, as can be the subfamily $\mathcal{F}_1$ corresponding to CALC or the subfamily $\mathcal{F}_2$ considered in [12].

COROLLARY 3.2. *Assume that* (C1)–(C4) *hold. A boundary collision bifurcation of the period adding structure of CALC occurs if and only if there exist* $\lambda \in (0,1)$ *and* $m, n \in \mathbb{N}$ *with* $\gcd(m,n) = 1$ *such that* $h = \lambda^n$, $c = \lambda^m$, *and* $\lambda A_R \leq A_H$. *Moreover, both* A_H *and* A_R *are* $(m+n)$*-periodic and their orbits have* m *points in* $(0, A_H]$ *and* n *points in* $[A_R, +\infty)$.

In section 4 we will use Corollary 3.2 to determine the PAS of CALC for different population growth models describing the underlying dynamics. In the remainder of this subsection, we use Proposition 3.1 to complete the study of the PAS of $\mathcal{F}_2$ started in [12]. Following the notation in that paper, after imposing the parameter restrictions defining $\mathcal{F}_2$, we write the parameters of (3.1) in terms of $r \in (0,1)$ and $\epsilon > r$ in the form $a_\mathcal{L} = 1 + r$, $a_\mathcal{R} = 1 - r$, $d_\mathcal{L} = \epsilon/(\epsilon+r)$, and $d_\mathcal{R} = \epsilon/(\epsilon-r)$.

COROLLARY 3.3. *Consider* (3.1) *for* $a_\mathcal{L} = 1 + r$, $a_\mathcal{R} = 1 - r$, $d_\mathcal{L} = \epsilon/(\epsilon+r)$, *and* $d_\mathcal{R} = \epsilon/(\epsilon-r)$, *with* $r \in (0,1)$ *and* $\epsilon > r$. *Then, a boundary collision bifurcation of the period adding structure occurs if and only if there exist* $m, n \in \mathbb{N}$ *with* $\gcd(m,n) = 1$ *such that*

$$\begin{cases} (1+r)^m(1-r)^n = 1, \\ \epsilon \geq r\left(\frac{\sqrt[n]{1+r}+1}{\sqrt[n]{1+r}-1}\right). \end{cases} \tag{3.2}$$

Moreover, both $d_\mathcal{L}$ *and* $d_\mathcal{R}$ *are* $(m+n)$*-periodic and their orbits have* m *points in* $(0, \epsilon/(\epsilon+r)]$ *and* n *points in* $[\epsilon/(\epsilon-r), +\infty)$.

The period adding structure in the $r-\epsilon$ plane that can be derived from Corollary 3.3 is shown in Figure 5, which reproduces Figure 5a in [12] with two important

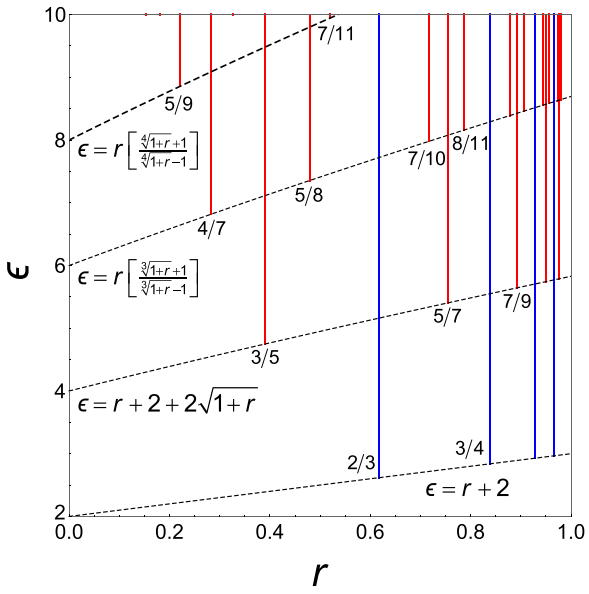

FIG. 5. *Period adding structure of* (3.1) *for* $a_{\mathcal{L}} = 1 + r$, $a_{\mathcal{R}} = 1 - r$, $d_{\mathcal{L}} = \epsilon/(\epsilon+r)$, *and* $d_{\mathcal{R}} = \epsilon/(\epsilon-r)$, *with* $r \in (0,1)$ *and* $\epsilon > r$. *This figure is analogous to Figure* 5a *in* [12], *except that the periodicity region of rotation number* $1/2$ *has been omitted and the endpoints of the different regions are analytically determined by Corollary* 3.3. *The curves containing these points are represented by dashed lines and the expression of each of them is indicated.*

differences. First, the periodicity region of rotation number $1/2$ that appears in [12] is not represented in Figure 5. The reason is that this region actually does not exist, since it corresponds to $r = 0$ and for that value the graph of the map reduces to the straight line $y = x$. Second, in [12] the endpoints of the periodicity regions were only determined for Leonov's first complexity level (blue lines in Figure 5), which in this case correspond to $n = 1$. Specifically, in [12] it was proved by using the skew tent map as normal form that the endpoints of the periodicity regions for the first complexity level are on the line $\epsilon = r + 2$. The same conclusion can be directly drawn by substituting $n = 1$ in the second condition of Corollary 3.3. For the remaining periodicity regions (i.e., $n \geq 2$), no expressions for the endpoints were provided in [12] and it was only stated that all of them are above the line $\epsilon = r + 2$. The second condition in Corollary 3.3 provides the exact values of the endpoints for all complexity levels and completes the analytical determination of the PAS of the family of maps considered in [12]. The curves containing these endpoints are represented by dashed lines in Figure 5 and the analytical expression of each of them is indicated.

3.3. Degenerate border collision bifurcations. Apart from determining the PAS of $\mathcal{F}_0$ (and, in particular, of CALC), Proposition 3.1 reveals another relevant fact: when a BCB of the PAS occurs, the two kink points of the map collide at the same time with cycles in the outermost partitions of the state space and that have the same rotation number. This suggests that the BCBs for the family of maps $\mathcal{F}_0$ are different from the ones that have been previously observed for $\mathcal{F} \setminus \mathcal{F}_0$ [29, 30, 31] and constitute a rather degenerate case. For any fixed parameter point inside one of the periodicity regions of the PAS of $\mathcal{F} \setminus \mathcal{F}_0$ there exists a unique cycle associated with it, which can be attracting or not [29]. In particular, at a bifurcation point the unique cycle that exists may contain either $d_{\mathcal{L}}$ or $d_{\mathcal{R}}$. In the case of $\mathcal{F}_0$, by Proposition 3.1

we know that at any bifurcation point there exist, at least, two different cycles with the same rotation number when the parameters satisfy $\lambda d_{\mathcal{R}} < d_{\mathcal{L}}$, one containing $d_{\mathcal{L}}$ and another containing $d_{\mathcal{R}}$. Apart from giving us a glimpse of the degeneracy of the case, this difference leads to the question about the exact number of cycles with the same rotation number that may exist at a bifurcation point of $\mathcal{F}_0$.

Beyond the theoretical interest of this question, it is also relevant from a practical point of view in the case of CALC. Managers could be particularly interested in avoiding control intensities corresponding to bifurcation points in light of the problems that small variations of the parameters around these points may cause. However, in case we were faced with one of these bifurcations, it would be of practical interest to know in advance how the managed populations would behave.

To illustrate the dynamical behavior at bifurcation points of the PAS of maps of $\mathcal{F}_0$ and compare that behavior to what is known for $\mathcal{F} \setminus \mathcal{F}_0$, we consider the maps $f_1 \in \mathcal{F} \setminus \mathcal{F}_0$ and $f_2 \in \mathcal{F}_0$ given by

$$
\begin{aligned}
f_1(x) &= \begin{cases} 2x+2, & x \le 1, \\ (2\alpha - 4.5)x + 8.5 - 2\alpha, & 1 < x < 2, \\ \alpha x - 0.5, & x \ge 2, \end{cases} \\
f_2(x) &= \begin{cases} 3x, & x \le 1, \\ (2\alpha - 3)x + 6 - 2\alpha, & 1 < x < 2, \\ \alpha x, & x \ge 2, \end{cases}
\end{aligned} \tag{3.3}
$$

with $\alpha \in (0,1)$. It is routine to check that a bifurcation of the PAS of f_1 occurs for $\alpha = 3/8$. For this value, the graph of f_1 together with its second iterate $f_1^2 = f_1 \circ f_1$ is shown in Figure 6(a). In this case, the bifurcation occurs by the collision of $d_{\mathcal{L}} = 1$ with a cycle of rotation number $1/2$, while the other kink point of the map, $d_{\mathcal{R}} = 2$, is not 2-periodic. In fact, $d_{\mathcal{R}}$ collides with a cycle of the same rotation number for a lower value of α, namely $\alpha = 1/4$. The parameter interval between these two bifurcation points, $(1/4, 3/8)$, corresponds to the periodicity region of rotation number $1/2$. For all parameter values inside that interval a unique 2-cycle exists, which lies in $I_{\mathcal{L}} \cup I_{\mathcal{R}}$ and in this case is globally attracting as Figure 6(b) shows. The most important aspect, however, is that no abrupt change in the magnitude of the state variable occurs when α is varied through the bifurcation point. The situation is completely different for f_2. For this map, a bifurcation of the PAS associated with cycles of rotation number $1/2$ occurs for $\alpha = 1/3$. As shown in Figure 6(c) and in line with Proposition 3.1, for that parameter value the two kink points of the map collide simultaneously with cycles of that rotation number. Yet, not only the two break points of the map become periodic at the bifurcation point, but a continuum of cycles with all their points lying in $I_{\mathcal{L}} \cup I_{\mathcal{R}}$ and with the same rotation number $1/2$ exist. Two important facts about these cycles can be observed in Figure 6(d). First, these infinitely many 2-cycles do not exist for values of parameter α on either side of the bifurcation point. Second, when α is varied through the bifurcation point the magnitude of the state variable undergoes a sharp shift between two different attractors, which are connected by the continuum of 2-cycles. This is the same behavior that was observed for CALC in section 2.

This example illustrates the differences between the bifurcations of the PAS for maps in $\mathcal{F}_0$ and those in $\mathcal{F} \setminus \mathcal{F}_0$. In the following result we prove that the behavior described in the example is generic for maps in $\mathcal{F}_0$.

PROPOSITION 3.4. *Consider* (3.1) *for* $\mu_{\mathcal{L}} = \mu_{\mathcal{R}} = 0$. *Assume that there exist* $\lambda \in (0,1)$ *and* $m, n \in \mathbb{N}$ *with* $\gcd(m,n) = 1$ *such that* $a_{\mathcal{L}} = \lambda^{-n}$, $a_{\mathcal{R}} = \lambda^m$, *and* $\lambda d_{\mathcal{R}} \le d_{\mathcal{L}}$. *Then, the following holds:*

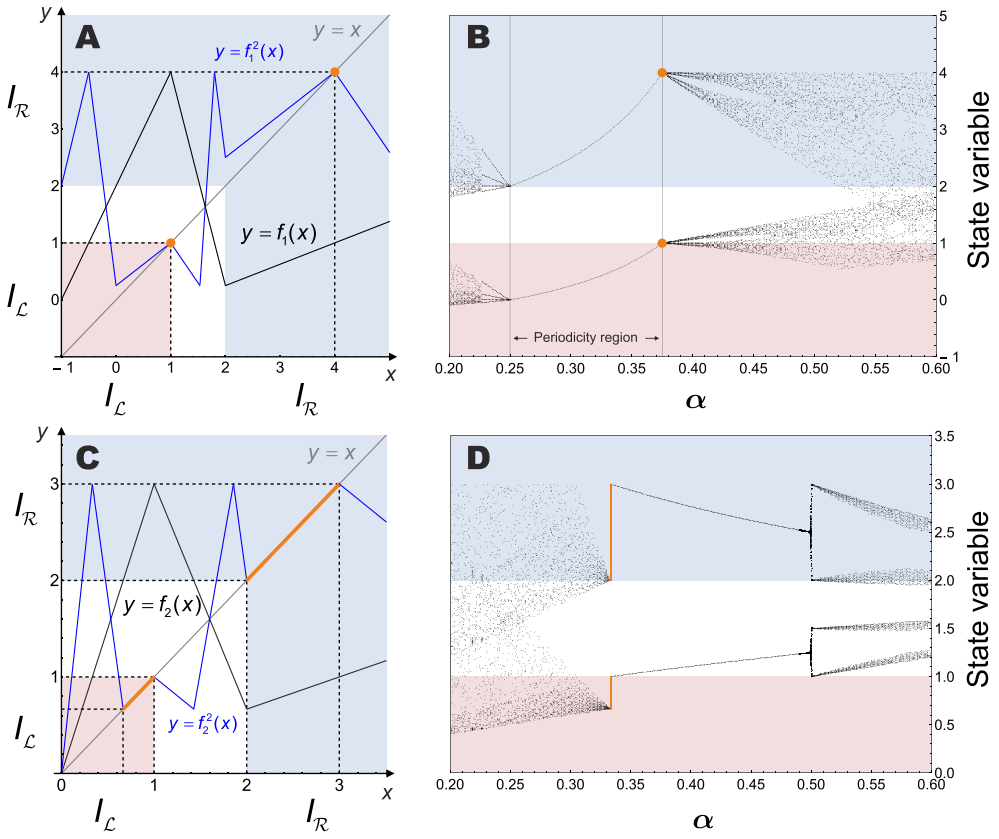

FIG. 6. (a) *Graphical representation of* f_1 *in* (3.3) *and its second iterate* $f_1^2 = f_1 \circ f_1$ *for* $\alpha = 3/8$. (b) *Bifurcation diagram of* f_1 *in* (3.3) *for varying* α. (c) *Graphical representation of* f_2 *in* (3.3) *and its second iterate* $f_2^2 = f_2 \circ f_2$ *for* $\alpha = 1/3$. (d) *Bifurcation diagram of* f_2 *in* (3.3) *for varying* α. *In all panels, the orange points correspond to* 2*-cycles associated with BCBs of the period adding structure, the red area corresponds to the interval* $I_{\mathcal{L}}$, *and the blue area corresponds to* $I_{\mathcal{R}}$.

(i) *If* $\lambda d_{\mathcal{R}} < d_{\mathcal{L}}$, *all points in*

$$\mathcal{B} = \bigcup_{i=-n}^{m-1} [\lambda^{i+1} d_{\mathcal{R}}, \lambda^i d_{\mathcal{L}}]$$

are $(m+n)$*-periodic and their orbits have* m *points in* $I_{\mathcal{L}}$ *and* n *points in* $I_{\mathcal{R}}$.

(ii) *If* $\lambda d_{\mathcal{R}} = d_{\mathcal{L}}$, $d_{\mathcal{L}}$ *and* $d_{\mathcal{R}}$ *belong to the same periodic orbit of period* $m+n$ *with* m *points in* $I_{\mathcal{L}}$ *and* n *points in* $I_{\mathcal{R}}$.

Proof. Assume $\lambda d_{\mathcal{R}} < d_{\mathcal{L}}$. Under this condition, $\mathcal{B}$ is a well-defined disjoint union of nonempty intervals. For $i \in \{-n, \dots, m-1\}$, denote $J_i = [\lambda^{i+1} d_{\mathcal{R}}, \lambda^i d_{\mathcal{L}}]$ and consider $\mathcal{B}_{\mathcal{L}} = \bigcup_{i=0}^{m-1} J_i$ and $\mathcal{B}_{\mathcal{R}} = \bigcup_{i=-n}^{-1} J_i$. With this notation, $\mathcal{B} = \mathcal{B}_{\mathcal{L}} \cup \mathcal{B}_{\mathcal{R}}$, $\mathcal{B}_{\mathcal{L}} \cap \mathcal{B}_{\mathcal{R}} = \emptyset$, $\mathcal{B}_{\mathcal{L}} \subset I_{\mathcal{L}}$, and $\mathcal{B}_{\mathcal{R}} \subset I_{\mathcal{R}}$. Given that $\lambda < 1$, $F(x) = F_{\mathcal{L}}(x) = \lambda^{-n} x > x$ for $x \in \mathcal{B}_{\mathcal{L}}$ and $F(x) = F_{\mathcal{R}}(x) = \lambda^m x < x$ for $x \in \mathcal{B}_{\mathcal{R}}$. Besides, $F(\max \mathcal{B}_{\mathcal{L}}) = F(d_{\mathcal{L}}) = \lambda^{-n} d_{\mathcal{L}} = \max \mathcal{B}$ and $F(\min \mathcal{B}_{\mathcal{R}}) = F(d_{\mathcal{R}}) = \lambda^m d_{\mathcal{R}} = \min \mathcal{B}$. With these conditions, $F(\mathcal{B}) \subset [\min \mathcal{B}, \max \mathcal{B}]$. On the other hand, F is a bijection between J_i

and J_{i-n} for $i \in \{0, \dots, m-1\}$ and between J_i and J_{i+m} for $i \in \{-n, \dots, -1\}$. This proves that $\mathcal{B}$ is an invariant set for F and that the application of F to any point in $\mathcal{B}$ leads to another point in a different component of $\mathcal{B}$.

Suppose now that $F^q(J_i) = J_i$ for certain $i \in \{-n, \dots, m-1\}$ and $q \in \mathbb{N}$. Since $\mathcal{B}$ is F-invariant and bijects components of $\mathcal{B}$ into different components of $\mathcal{B}$, the q intervals $J_i, F(J_i), \dots, F^{q-1}(J_i)$ correspond to components of $\mathcal{B}$. Assume that $\tilde{m}$ of these intervals lie in $B_{\mathcal{L}}$ and $\tilde{n}$ in $B_{\mathcal{R}}$. Then, by the commutativity between $F_{\mathcal{L}}$ and $F_{\mathcal{R}}$ it follows that $F^q(J_i) = \lambda^{m\tilde{n}-n\tilde{m}} J_i = J_i$, which implies $m\tilde{n} = n\tilde{m}$. Under the coprimality condition for m and n, this equality is only possible if $\tilde{m}$ is a multiple of m and $\tilde{n}$ is a multiple of n. Assume that $\tilde{m} = km$ for a certain $k \in \mathbb{N}$. Then, $\tilde{n} = kn$ and $q = \tilde{m}+\tilde{n} = k(m+n) \geq m+n$. This means that for any $i \in \{-n, \dots, m-1\}$ the $m+n$ intervals $J_i, F(J_i), \dots, F^{m+n-1}(J_i)$ are different, and thus they correspond to each of the components of $\mathcal{B}$. Since $\mathcal{B}$ has m components in $B_{\mathcal{L}}$ and n components in $B_{\mathcal{R}}$, again by the commutativity of $F_{\mathcal{L}}$ and $F_{\mathcal{R}}$ we obtain $F^{m+n}(J_i) = \lambda^{mn-nm} J_i = J_i$. This proves that all the points of $\mathcal{B}$ are $(m+n)$-periodic and that their orbits have m points in $I_{\mathcal{L}}$ and n points in $I_{\mathcal{R}}$.

Assume now that $\lambda d_{\mathcal{R}} = d_{\mathcal{R}}$. According to Proposition 3.1, a BCB occurs for the control intensities given in Proposition 3.4 and both break points $d_{\mathcal{L}}$ and $d_{\mathcal{R}}$ are $(m+n)$-periodic. Moreover, in the proof of Proposition 3.1 it was shown that under the conditions in Proposition 3.4 the point $\lambda d_{\mathcal{R}}$ is in the same cycle as $d_{\mathcal{R}}$, which completes the proof. ∎

Proposition 3.4 allows us to obtain a full picture of the degenerate BCBs considered here. No cycles lying in the outermost partitions of the state space exist for parameter values outside the periodicity regions of $\mathcal{F}_0$. Since these regions have zero Lebesgue measure in the parameter space and coincide with the bifurcation manifolds, when parameters cross one of them a continuum of cycles lying in the outermost partitions of the state space emerge at the bifurcation point and disappear afterward. This is what was observed for the map f_2 in the previous example (cf. Figure 6(d)).

Remark 3.5. Two important facts must be stressed about Proposition 3.4 in the case of CALC. First, notice that the results provided in this proposition are independent of the expression of the map between the two kink points. In the case of CALC, this means that the population map f plays no role in the dynamics at bifurcation points of the PAS. Yet, according to Corollary 3.2, bifurcations of the PAS only occur for $\lambda A_R \leq A_H$ with $c = \lambda^n$, $h = \lambda^m$, and n, m coprime, and we know that in that case the break points A_R and A_H are determined in terms of f by the equations $f(A_R) = \lambda^m A_R$ and $f(A_H) = \lambda^n A_H$. Consequently, although f plays no role in the dynamics at the bifurcation points, it determines the number of bifurcations that can occur and the combination of control intensities corresponding to them. Second, parameters m and n in Proposition 3.4 have a specific meaning in the case of CALC. They represent, respectively, the number of harvesting and restocking episodes that are necessary to complete one of the cycles associated with BCBs if we consider a point of the cycle as the initial condition. This result may be helpful to predict the population behavior in the case of facing such a bifurcation. Moreover, according to Corollary 3.2, when a BCB of CALC occurs the equality $c^n = h^m$ holds. For $c > h$ we have $c^n = h^m > h^n$, and thus $m < n$. Therefore, when at a bifurcation point the restocking intensity is higher than the harvesting intensity, the number of restocking episodes associated with the cycles of that bifurcation is larger than the number of harvesting episodes. By the same argument, it can be seen that the opposite occurs for $c < h$.

4. Examples. In this section we use the theoretical results provided in the previous section to determine the period adding structure of CALC for two well-known production maps. These examples show that this structure may range from very simple to very intricate depending on the map that is considered.

4.1. Ricker model. We start by considering the Ricker map $f(x) = x\exp(r(1-x/K))$ with $r = 3$ and $K = 60$. Using Corollary 3.2, only two BCBs can occur for this map, namely for $c = h \gtrsim 0.076$ and $c^{1/2} = h \gtrsim 0.117$. These two bifurcations can be observed in the bifurcation diagram of Figure 3, where c is set at 0.6 and h is varied. For $c = h = 0.6$, the inequality $cA_R < A_H$ holds and an infinite number of 2-cycles are predicted by Proposition 3.4. These cycles have one point in $I_{\mathcal{L}}$ and another point in $I_{\mathcal{R}}$ and completely fill $\mathcal{B} = [cA_R, A_H] \cup [A_R, A_H/c] \approxeq [42.13, 49.78] \cup [70.22, 82.97]$. They correspond to the orange dots in Figure 3. The dynamics of these cycles is based on alternating episodes of restocking and harvesting as the number of individuals switches between the two components of $\mathcal{B}$.

Similarly, for $c = h^2 = 0.6$ the inequality $\sqrt{c}A_R < A_H$ holds and a continuum of 3-cycles is predicted by Proposition 3.4. These cycles have two points in $I_{\mathcal{L}}$ and one point in $I_{\mathcal{R}}$ and fill $\mathcal{B} = [cA_R, \sqrt{c}A_H] \cup [\sqrt{c}A_R, A_H] \cup [A_R, A_H/\sqrt{c}] \approxeq [42.13, 42.52] \cup [54.39, 54.89] \cup [70.22, 70.86]$. They correspond to the green dots in Figure 3. The dynamics of these cycles is based on a succession of three control episodes, which consist of two consecutive episodes of harvesting followed by one episode of restocking.

At the two bifurcation points the continuum of cycles seems to attract all orbits except those corresponding to fixed points. Thus, the managed populations asymptotically behave as has been described for these cycles.

From the practical point of view, if only two BCBs occur as in this example it may be possible to implement the control in such a way that sharp changes in the dynamics can be avoided (and thus, the problems associated with them). However, the number of BCBs that can occur strongly depends on the production function for the uncontrolled population. This number can be very large, as we illustrate in the following subsection. In such a case, avoiding the negative effects of BCBs can be particularly difficult.

4.2. Hassell model. As stated in Remark 3.5, the number of bifurcations of the PAS of CALC depends on the population map f. The steeper this map is around the positive fixed point of the production function, the closer A_R and A_H are for a fixed λ satisfying $c = \lambda^m$ and $h = \lambda^n$ for coprime $m, n \in \mathbb{N}$ (recall that $f(A_R) = \lambda^m A_R$ and $f(A_H) = \lambda^{-n} A_H$). Consequently, there are more chances for the existence of values of λ satisfying $\lambda A_R \leq A_H$ and, according to Corollary 3.2, more combinations of control intensities can correspond to bifurcation points. In view of this, we consider the Hassell map [18]

$$x_{t+1} = \frac{Ax_t}{(1 + Bx_t)^{\alpha}}$$

with $A = 1000$, $B = 0.05$, and $\alpha = 50$. For these parameter values, the modulus of the derivative of the production function around the carrying capacity is large, namely approximately 8.20. Using Corollary 3.2, the PAS of CALC for this production function was determined and is shown in Figure 7. Up to period 10, a total of 29 BCBs can occur for different values of the parameters. This demonstrates that the number of bifurcations of the PAS of CALC can be very high, as well as the period of the corresponding cycles. This may have severe consequences on the applicability of CALC, as shown in Figure 8, where the bifurcation diagram of CALC for this last

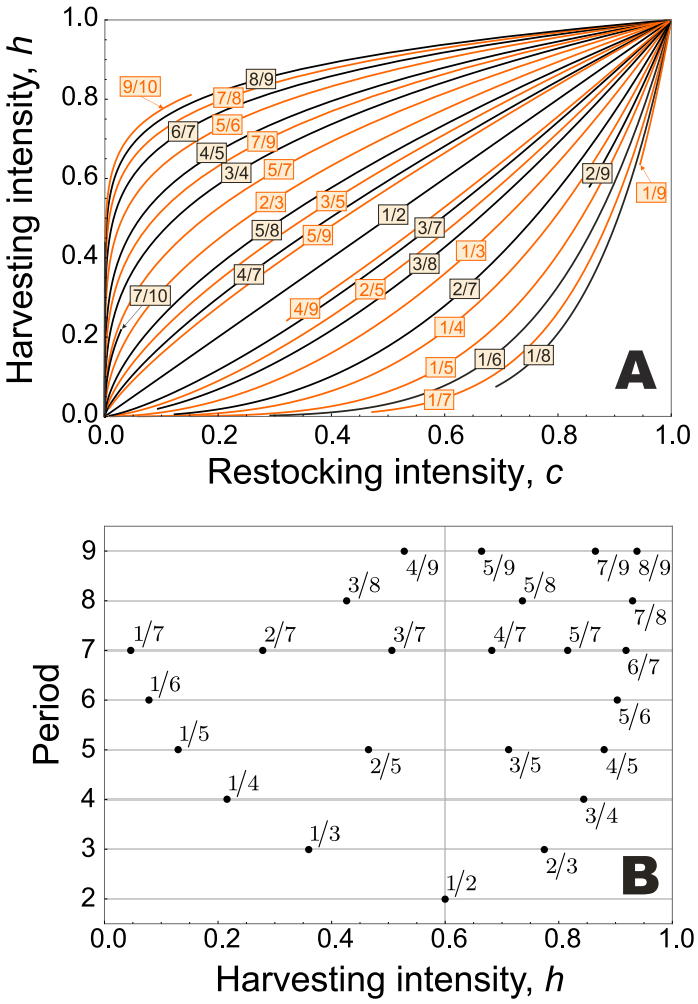

FIG. 7. (a) *Period adding structure of CALC.* (b) *Distribution of periods of the period adding structure of CALC for* $c = 0.6$ *and varying* h. *Each point is labeled in the form* $m/(m+n)$, *where* m *denotes the number of points of the cycles in* $I_{\mathcal{L}}$ *and* n *the number of points in* $I_{\mathcal{R}}$. *Both panels are based on the Hassell map* $f(x) = Ax/(1+Bx)^{\alpha}$ *with* $A = 1000$, $B = 0.05$, *and* $\alpha = 50$. *In panel* (a) *two colors are used to help distinguish different curves.*

example with $c = 0.6$ and varying h is represented. As can be observed, the distance between harvesting intensities of consecutive bifurcation points is short.

This last example demonstrates the practical relevance of Proposition 3.1. Without it, if only the necessary condition for the occurrence of BCBs obtained in [12] was used, the difficulties in the application of CALC would be even greater than in this last example for all population maps, including the Ricker model considered in the first example. The reason for this is that for managers it may be hard to know which combinations of control intensities satisfying $c^m h^n = 1$ for coprime $m, n \in \mathbb{N}$ actually are bifurcation points and which ones are not. In that case, up to period 10, when fixing one of the control intensities a total of 31 potential bifurcation points would be obtained for the other control intensity in an interval of length 1. This would make it difficult to find a combination of control intensities with guarantees of placing the population away from any bifurcation point.

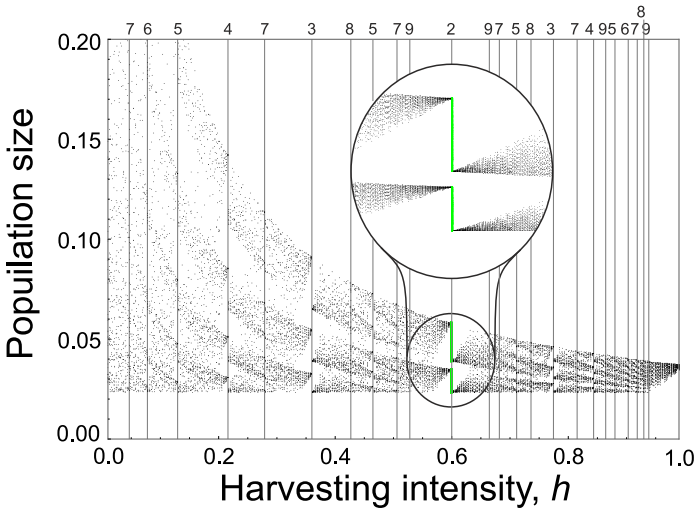

FIG. 8. *Bifurcation diagram for CALC with* $c = 0.6$ *and varying* h *based on the Hassell map* $f(x) = {}^{Ax}/_{(1+Bx)^{\alpha}}$ *with* $A = 1000$, $B = 0.05$, *and* $\alpha = 50$. *For each value of* h, *black dots represent* 30 *iterates of the state variable after a transient of* 10,000 *iterates with initial conditions obtained as pseudorandom real numbers in the interval* $(0, f(d)]$. *The vertical lines represent the harvesting intensities for which BCBs occur according to Corollary* 3.2, *and the numbers above them indicate the period of the cycles given by Proposition* 3.4. *For* $h = 0.6$, *iterates were obtained for* 1,000 *different initial conditions, which are represented by green dots.*

5. Discussion and conclusions. The study presented here is motivated by an application in population dynamics. We have considered CALC as a method for the control of biological populations aimed at reducing the fluctuations in the population size. This strategy corresponds to the combination of two already known control methods, namely adaptive limiter control and adaptive threshold harvesting, of which the former is based on restocking the population size and the latter constitutes its harvesting version. In the analysis of CALC we observe abrupt transitions in the dynamics of the managed populations that do not occur when only restocking or only harvesting is implemented.

We provide numerical simulations showing potential risks and opportunities associated with these changes in the dynamics. On the one hand, the number of individuals undergoes sharp shifts between different attractors, which may seriously affect the stability and persistence of the population. This can be a serious problem in the case of endangered or commercially exploited species but an opportunity in the case of nuisance or invasive species. On the other hand, transitions between different attractors are coupled with abrupt changes in the type of control prevailing in the intervention (restocking or harvesting). Again, this can be a problem as long as the yield, cost, and logistics of the exploitation can be seriously affected. Yet, it can also be beneficial. When it is very costly to restock a population, it can be interesting to lead the population toward the side of the bifurcation point corresponding to the attractor for which a lower number of individuals have to be restocked.

The theoretical analysis of these phenomena leads to a mathematical problem concerning nonsmooth discrete dynamical systems. When the underlying dynamics are described by unimodal maps, we have shown that the production function of CALC is piecewise continuous with two angular points that divide the state space into three intervals. This function is linear on the extreme partitions of its domain

and is completely determined over them by the control intensities. The abrupt changes in the population dynamics are caused by the collision of periodic orbits lying in the outermost partitions of the state space with the break points of the CALC map. When only the external branches of this map are considered, it can be seen in terms of the control intensities as a biparametric family of bimodal PWL maps. We have shown that this family can be derived via certain parameter restrictions from a more generic six-parametric family of PWL maps, for which different bifurcation structures have been described in the literature [29, 30, 31]. Among these structures, the focus is on the so-called period adding structure, since it corresponds to bifurcations involving events that occur only in the outermost partitions of the state space.

Similar considerations were previously done in [12] for another biparametric family of PWL maps. This family has in common with CALC that the maps are purely linear on the extreme partitions of their domain. An insightful description of the bifurcation structure of this family of maps was obtained in [12] by direct substitution of the parameter restrictions in the already known bifurcation structure for the generic six-parametric family of PWL maps. However, only partial results were obtained. We have shown that the imposition of the conditions for the homogeneity of the outermost branches of the map induces a degeneracy in the PAS that makes it impossible to relate the different structures via direct substitution of the parameter restrictions. We have proved that the inclusion of an additional condition involving the break points of the map resolves the indetermination in the PAS caused by this degeneracy. This allows us to fully determine the PAS of any family of maps with the extreme branches purely linear, e.g., CALC or the family of maps considered in [12].

Examples of the application of these theoretical results to the determination and description of the PAS of CALC for some models common in population dynamics are provided. These examples show that the number of BCBs strongly depends on the production function of the uncontrolled population, and thus the range of possibilities is wide.

We have also studied the degenerate BCBs that occur when homogeneity is imposed for the outermost branches of the map. We have proved that when parameters are varied through one of the bifurcation points, a continuum of cycles lying in the external partitions of the state space emerge and disappear afterward. Moreover, we have obtained analytical results for the endpoints of the intervals filled by these cycles. These results are independent of the functional expression of the map in the middle partition of the domain and thus are applicable to CALC with any unimodal growth model for the uncontrolled population. Numerical simulations reveal that the state variable abruptly shifts between different attractors that are connected by the continuum of cycles that exist at the bifurcation points.

We point out that our study has focused on the bifurcation structure associated with collisions of the break points of PWL maps and cycles lying on the outermost partitions of their state space. Several reasons justify the focus on these partitions in the case of CALC. On the one hand, for overcompensatory population maps with unstable equilibrium the state variable is expected to enter these partitions after a certain time if the control intensities are high enough. On the other hand, the outermost partitions are more relevant in cases in which the population size is rather small or large, respectively corresponding to scenarios close to extinctions or outbreaks. For the general case of 1D bimodal PWL maps, bifurcation structures associated with border collisions of invariant sets lying totally or partially on the central partition of the state space have been deeply studied (see, e.g., [29, 30, 31]). Yet, these results cannot be applied to CALC since the central branch of the CALC map is assumed

to be nonlinear. Studying border collisions of invariant sets containing points in the central partition of CALC and their possible ecological and management implications is an interesting open problem to be addressed in future research.

REFERENCES

[1] V. S. Anishchenko, T. E. Vadivasova, and G. I. Strelkova, *Deterministic Nonlinear Systems. A Short Course*, Springer, Berlin, 2014.

[2] M. J. Armstrong, *An analysis of yield variability from three harvesting strategies in the South African anchovy fishery, under conditions of randomly fluctuating recruitment success*, S. Afr. J. Marine Sci., 2 (1984), pp. 131–144.

[3] V. Avrutin, L. Gardini, I. Sushko, and F. Tramontana, *Continuous and Discontinuous Piecewise-Smooth One-Dimensional Maps*, World Scientific, River Edge, NJ, 2019.

[4] V. Avrutin and I. Sushko, *A gallery of bifurcation scenarios in piecewise smooth* 1*D maps*, in Global Analysis of Dynamic Models in Economics and Finance, G. Bischi G, C. Chiarella and I. Sushko, eds., Springer, Berlin, 2013, pp. 369–395.

[5] V. Avrutin, I. Sushko, and F. Tramontana, *Bifurcation structure in a bimodal piecewise linear business cycle model*, Abstr. Appl. Anal., 2014 (2014), 401319.

[6] J. R. Beddington and R. M. May, *Harvesting natural populations in a randomly fluctuating environment*, Science, 197 (1977), pp. 463–465.

[7] T. S. Bellows, *The descriptive properties of some models for density dependence*, J. Anim. Ecol., 50 (1981), pp. 139–156.

[8] M. Bernardo, C. Budd, A. R. Champneys, and P. Kowalczyk, *Piecewise-Smooth Dynamical Systems: Theory and Applications*, Springer, Berlin, 2008.

[9] M. D. Bernardo, C. Budd, A. R. Champneys, P. Kowalczyk, A. B. Nordmark, G. O. Tost, and P. T. Piiroinen, *Bifurcations in nonsmooth dynamical systems*, SIAM Rev., 50 (2008), pp. 629–701.

[10] H. M. Chang and J. Juang, *Piecewise two-dimensional maps and applications to cellular neural networks*, Internat. J. Bifur. Chaos Appl. Sci. Engrg., 14 (2004), pp. 2223–2228.

[11] S. Dey and A. Joshi, *Effects of constant immigration on the dynamics and persistence of stable and unstable* Drosophila *populations*, Sci. Rep., 3 (2013), 1405.

[12] I. Foroni, A. Avellone, and A. Panchuk, *Sudden transition from equilibrium stability to chaotic dynamics in a cautious tâtonnement model*, Chaos Solitons Fractals, 79 (2015), pp. 105–115.

[13] D. Fournier-Prunaret and P. Chargé, *Route to chaos in a circuit modeled by a* 1*-dimensional piecewise linear map*, NOLTA, 3 (2012), pp. 521–532.

[14] D. Franco and F. M. Hilker, *Adaptive limiter control of unimodal population maps*, J. Theoret. Biol., 337 (2013), pp. 161–173.

[15] D. Franco and F. M. Hilker, *Stabilizing populations with adaptive limiters: Prospects and fallacies*, SIAM J. Appl. Dyn. Syst., 13 (2014), pp. 447–465.

[16] L. Gardini, T. Puu, and I. Sushko, *A Goodwin-type model with a piecewise linear investment function*, in Business Cycle Dynamics, T. Puu and I. Sushko, eds., Springer, Berlin, 2006.

[17] L. Gardini, F. Tramontana, and I. Sushko, *Border collision bifurcations in one-dimensional linear-hyperbolic maps*, Math. Comput. Simul., 81 (2010), pp. 899–914.

[18] M. P. Hassell, *Density-dependence in single-species populations*, J. Anim. Ecol., 44 (1975), pp. 283–295.

[19] F. M. Hilker and F. H. Westerhoff, *Control of chaotic population dynamics: Ecological and economic considerations*, Beitraege Inst. Umweltsystemforschung, 32 (2005), pp. 1–21.

[20] F. M. Hilker and F. H. Westerhoff, *Preventing extinction and outbreaks in chaotic populations*, Am. Nat., 170 (2007), pp. 232–241.

[21] J. Juang, C. Li, and M. Liu, *Cellular neural networks: Mosaic patterns, bifurcation and complexity*, Internat. J. Bifur. Chaos Appl. Sci. Engrg., 16 (2006), pp. 47–57.

[22] T. Kousaka and H. Asahara, *Complete bifurcation analysis of a chaotic attractor in an electric circuit with piecewise-smooth characteristics*, IEEJ Trans. Electr. Electr., 9 (2014), pp. 656–663.

[23] M. Kunze, *Non-smooth Dynamical Systems*, Lecture Notes in Math. 1744, Springer, Berlin, 2000.

[24] R. Lande, B. Sæther, and S. Engen, *Threshold harvesting for sustainability of fluctuating resources*, Ecology, 78 (1997), pp. 1341–1350.

[25] N. N. Leonov, *Map of the line onto itself*, Radiofiz., 3 (1959), pp. 942–956.

[26] X. Li., *Analysis of complete stability for discrete-time cellular neural networks with piecewise linear output functions*, Neural Comput., 21 (2009), pp. 1434–1458.
[27] S. A. Murawski and J. S. Idoine, *Yield sustainability under constant-catch policy and stochastic recruitment*, Trans. Am. Fish. Soc., 118 (1989), pp. 349–367.
[28] H. E. Nusse and J. A. Yorke, *Border-collision bifurcations including "period two to period three" for piecewise smooth systems*, Phys. D, 57 (1992), pp. 39–57.
[29] A. Panchuk, I. Sushko, and V. Avrutin, *Bifurcation structures in a bimodal piecewise linear map: chaotic dynamics*, Internat. J. Bifur. Chaos Appl. Sci. Engrg., 25 (2015), 1530006.
[30] A. Panchuk, I. Sushko, and V. Avrutin, *Bifurcation structures in a bimodal piecewise linear map*, Front. Appl. Math. Stat., 3 (2017).
[31] A. Panchuk, I. Sushko, B. Schenke, and V. Avrutin, *Bifurcation structures in a bimodal piecewise linear map: regular dynamics*, Internat. J. Bifur. Chaos Appl. Sci. Engrg., 23 (2013), p. 1330040.
[32] W. E. Ricker, *Stock and recruitment*, J. Fish. Res. Board Can., 11 (1954), pp. 559–623.
[33] P. Sah and S. Dey, *Stabilizing spatially-structured populations through adaptive limiter control*, PloS One, 9 (2014), e105861.
[34] P. Sah, J. P. Salve, and S. Dey, *Stabilizing biological populations and metapopulations through adaptive limiter control*, J. Theoret. Biol., 320 (2013), pp. 113–123.
[35] J. Segura, F. M. Hilker, and D. Franco, *Adaptive threshold harvesting and the suppression of transients*, J. Theoret. Biol., 395 (2016), pp. 103–114.
[36] J. Segura, F. M. Hilker, and D. Franco, *Population control methods in stochastic extinction and outbreak scenarios*, PloS One, 12 (2017), e0170837.
[37] J. Segura, F. M. Hilker, and D. Franco, *Enhancing population stability with combined adaptive limiter control and finding the optimal harvesting–restocking balance*, Theor. Popul. Biol., 130 (2019), pp. 1–12.
[38] D. W. Skagen, *Management strategies for reducing variation in annual yield: When can they work?*, ICES J. Mar. Sci., 64 (2007), pp. 698–701.
[39] I. Sushko and L. Gardini, *Degenerate bifurcations and border collisions in piecewise smooth 1D and 2D maps*, Internat. J. Bifur. Chaos Appl. Sci. Engrg., 20 (2010), pp. 2045–2070.
[40] I. Sushko, L. Gardini, and K. Matsuyama, *Robust chaos in a credit cycle model defined by a one-dimensional piecewise smooth map*, Chaos Solitons Fractals, 91 (2016), pp. 299–309.
[41] F. Tramontana, L. Gardini, V. Avrutin, and M. Schanz, *Period adding in piecewise linear maps with two discontinuities*, Internat. J. Bifur. Chaos Appl. Sci. Engrg., 22 (2012), p. 1250068.
[42] S. Tung, A. Mishra, and S. Dey, *A comparison of six methods for stabilizing population dynamics*, J. Theoret. Biol., 356 (2014), pp. 163–173.
[43] S. Tung, A. Mishra, and S. Dey, *Simultaneous enhancement of multiple stability properties using two-parameter control methods in* Drosophila melanogaster, Ecol. Complex., 26 (2016), pp. 128–136.
[44] G. Zhong and F. Ayrom, *Periodicity and chaos in Chua's circuit*, IEEE Trans. Circuits Syst., 32 (1985), pp. 501–503.